ELSEVIER

Journal of Magnetism and Magnetic Materials 189 (1998) 283–292

Journal of magnetism and magnetic materials

Crystallographic and magnetic properties of $UFe_{5.8}Al_{6.2}$ single crystals

A.P. Gonçalves[a], P. Estrela[b], J.C. Waerenborgh[a], J.A. Paixão[c], M. Bonnet[d], J.C. Spirlet[e], M. Godinho[b], M. Almeida[a,*]

[a] *Departamento de Química, Instituto Tecnológico e Nuclear, P-2686 Sacavém Codex, Portugal*
[b] *Departamento de Física, Faculdade de Ciências da Universidade de Lisboa, Campo Grande ed. C1, P-1700 Lisboa, Portugal*
[c] *Departamento de Física da Universidade de Coimbra, Faculdade de Ciências e Tecnologia, P-3000 Coimbra, Portugal*
[d] *CEA-Départemant de Recherche Fondamentale sur la Matière Condensée, SPSMS, F-38054 Grenoble Cedex 9, France*
[e] *European Commission, Joint Research Centre, Institute for Transuranium Elements, Postfach 2340, D-76125 Karlsruhe, Germany*

Received 20 February 1998; received in revised form 18 June 1998

Abstract

Single crystals of $UFe_{5.8}Al_{6.2}$ were characterised by X-ray and neutron diffraction, ^{57}Fe Mössbauer spectroscopy and magnetisation. The structure refinement by X-ray and neutron diffraction shows a $ThMn_{12}$-type structure, the Fe atoms fully occupying the 8f and partially occupying the 8j positions. Mössbauer spectra confirm these occupations and further indicate a magnetic ordering below 293 K. Magnetisation measurements show a ferromagnetic behaviour below 300 K, with *a* and *b* as easy directions and a spontaneous magnetisation of 10.4 μ_B/f.u. at 5 K, due to the Fe occupation of 8j position. These single crystal results significantly differ from those previously obtained in UFe_6Al_6 polycrystalline samples obtained by melting and annealing.

PACS: 75.50.Cc

Keywords: $ThMn_{12}$-type structure; Uranium intermetallics; Magnetic intermetallics; Actinides; Magnetic anisotropy

1. Introduction

Compounds of f-elements with the $ThMn_{12}$-type structure and high iron content have recently been considered as good candidates for hard magnetic materials [1,2]. AFe_{12} (A = f-element) binary compounds do not exist since the partial substitution of iron by a third element being necessary to stabilise this type of structure.

One of the earliest studied family of compounds with the $ThMn_{12}$-type structure was the series $AFe_{12-x}Al_x$, with A = f-element, first studied on polycrystalline samples with rare-earth compounds [3,4], and later with actinides [5,6]. In these systems it was found that the aluminium concentration necessary to stabilise the structure is relatively high, usually more than 50%. The study of these

* Corresponding author. Tel.: 351 1 9550 021; fax: 351 1 9941 455; e-mail: malmeida@itn1.itn.pt.

0304-8853/98/$19.00
PII: S0304-8853(98)00253-4

low iron content compounds is important to a better understanding of the contribution from the different magnetic sublattices to the magnetism in this type of structure. These compounds present complex magnetic properties, even in cases such as LFe_4Al_8 (L = Y, Lu), where the iron atoms are located only in one crystallographic position (8f) and the f-element is nonmagnetic [7].

Studies in single crystals of UFe_4Al_8, showed an antiferromagnetic ordering of the iron sublattice and a ferromagnetic contribution due to the uranium atoms, below 150 K, with an unusual magnetisation process [8,9]. Previous measurements on UFe_6Al_6 powder samples indicate a ferromagnetic character [6,10]. Powder neutron diffraction results suggest that the iron moments in UFe_6Al_6 and UFe_5Al_7 are ordered in a configuration perpendicular to the c axis [10,11]. However, the study of magnetic and other physical properties in these samples was limited due to the lack of single crystals. In order to enable a more detailed study we envisaged the growth of single crystals. The $UFe_{12-x}Al_x$ phase diagram, previously explored by us, indicates a congruent melting composition range between $UFe_{3.8}Al_{8.2}$ and $UFe_{5.8}Al_{6.2}$ [12]. The UFe_6Al_6 composition does not melt congruently and these samples can only be obtained by thermal treatment of powder samples, that quite often are not monophasic. In this work X-ray and neutron diffraction, ^{57}Fe Mössbauer spectroscopy and single crystal magnetisation studies in $UFe_{5.8}Al_{6.2}$ are presented.

2. Experimental

Bulk charges for the $UFe_{5.8}Al_{6.2}$ crystal growth were prepared by melting in an induction furnace the stoichiometric amounts of the elements with purity of at least 99.9%. A small single crystal, with approximate dimensions $0.08 \times 0.09 \times 0.10\,mm^3$, was removed from the polycrystalline material, glued on the top of a glass fiber and transferred to a goniometer mounted on an Enraf-Nonius CAD-4 diffractometer with graphite monochromatised Mo K_α radiation ($\lambda = 0.71073$ Å).

The least-squares refinement of the 2θ values of 25 strong and well centred reflections from the various regions of the reciprocal space in the range $16.3^\circ < 2\theta < 38.2^\circ$ was used to obtain the unit-cell parameters.

The data set was collected at room temperature in an ω–2θ scan mode ($\Delta\omega = 0.80 + 0.35 \tan\theta$). Four reflections were monitored as orientation and three as intensity standards at 4 h intervals during the data collection; no variation larger than 0.5% was observed. The intensities of the 2288 measured reflections (with $2\theta < 80^\circ$) were corrected for absorption according to North et al. [13] and for polarisation and Lorentz effects. The equivalent reflections were averaged, resulting in 351 unique reflections from which 345 were considered significant ($I \geqslant 3\sigma(I)$).

The crystallographic structure was refined using the UPALS program [14]. Scattering factors for neutral atoms as well as anomalous dispersion corrections were taken from Ref. [15]. A type I isotropic secondary extinction correction (according to the Becker and Coppens formalism [16,17]) was refined, together with a scale factor, two position parameters (x for 8j and 8i crystallographic positions), two occupation factors and four isotropic temperature factors. The occupation by iron and aluminium atoms of the 8j and 8i positions was constrained to vary within the full site occupation. The least squares procedure converged to $R = \sum|F_{obs} - F_{calc}|/\sum|F_{obs}| = 0.052$ and $Rw = 0.064$ ($w = 1/\sigma^2$). Crystal data and experimental details of the structure determination are compiled in Table 1. Atomic positions, occupation factors and thermal displacement parameters are presented in Table 2.

Large single crystals aimed at neutron diffraction were grown from the bulk charges, using the Czochralski method, as previously described [12]. A small piece was removed from a single crystal, crushed, and used in X-ray powder diffraction in order to check for the existence of crystallographic superstructures that have been found in closely related compounds [18]. The crystals were aligned by X-ray diffraction in order to be used in the physical measurements.

A single crystal of approximate volume 15 mm^3 was examined by means of neutron-scattering. A data collection of Bragg intensities at room temperature was performed on the 4-circle instrument

Table 1
Crystal data and details of $UFe_{5.8}Al_{6.2}$ X-ray structure determination

Chemical formula	$UFe_{5.8}Al_{6.2}$
Formula weight	729.23 g/mol
Crystal system	Tetragonal
Space group [17]	I4/mmm (No.139)
a	8.6744(3) Å
c	5.0142(3) Å
V	377.30(5) Å^3
Z	2
D_{calc}	6.42 g cm^{-1}
μ(Mo K_α)	49.43 cm^2 g^{-1}
Approximate crystal dimensions	$0.09 \times 0.08 \times 0.10$ mm^3
Radiation, wavelenght	Mo K_α, 0.71073 Å
Monochromator	Graphite
Temperature	295 K
θ range	1.5–37°
ω–2θ scan	$\Delta\omega = 0.80 + 0.35 \tan\theta$
Data set	$-15 \leqslant h \leqslant 15,\ -15 \leqslant k \leqslant 15,\ -8 \leqslant l \leqslant 8$
Crystal-to-receiving-aperture distance	173 mm
Horizontal, vertical aperture	4, 4 mm
Total data	2288
Unique data	351
Observed data ($I \geqslant 3\sigma(I)$)	345
Number of refined parameters	10
Final agreement factors[a]	
$R = \sum\|F_{obs} - F_{calc}\|/\sum\|F_{obs}\|$	0.052
$wR = [\sum(w(\|F_{obs}\| - \|F_{calc}\|)^2)/w\|F_{obs}\|^2]^{1/2}$	0.064
$S = [\sum w(\|F_{obs}\| - \|F_{calc}\|)^2/(m-n)]^{1/2}$	1.561

[a] m: number of observations; n: number of variables.

Table 2
Atomic positions (x, y, z), occupation factors (OF) and temperature factors (U) obtained in the $UFe_{5.8}Al_{6.2}$ structure refinement from the X-ray data. The temperature factor is expressed as $T(\theta) = \exp[-8\pi^2 U(\sin\theta/\lambda)^2]$

Atom	Position	x	y	z	OF	$U \times 10^2$ (Å^2)
U	2a	0	0	0	1	0.51(2)
Fe	8f	1/4	1/4	1/4	1	0.51(3)
Fe	8j	0.2780(4)	1/2	0	0.36(3)	0.79(7)
Al	8j	0.2780(4)	1/2	0	0.64(3)	0.79(7)
Fe	8i	0.3447(5)	0	0	0.05(3)	0.85(9)
Al	8i	0.3447(5)	0	0	0.95(3)	0.85(3)

DN4 of the Siloë reactor at CEN-Grenoble. A neutron beam of wavelength 1.181 Å monochromated by reflection on the (0 0 2) face of a focusing Cu monochromator was used for this experiment. The estimated $\lambda/2$ contamination of the neutron beam at this wavelength is 5×10^{-3}. A total of 2762 reflections was measured, covering the angular range $11° \leqslant 2\theta \leqslant 120°$.

The comparison of the intensities of symmetry equivalent reflections has shown a poor agreement, particularly notorious for weaker reflections on the $l = 2n + 1$ layers. After testing that the crystal was

uniformly bathed by the beam and that no instrumental problem could possibly explain the bad agreement of the equivalent intensities we concluded that our crystal was probably not a single crystalline grain. A careful inspection of the intensity data has shown that indeed the crystal was a twin, with two grains (A, B) related by the following twin-law:

$$(h, k, l)_B = \begin{bmatrix} 1 & 0 & 0 \\ 0 & 1/2 & 1/2 \\ 0 & -1/2 & 1/2 \end{bmatrix} (h, k, l)_A.$$

This twin-law can be interpreted as follows. The cell parameters closely satisfy the condition $\sqrt{a^2 + c^2} = 2c$ ($a \approx \sqrt{3}c$), so that the interplanar spacing between the (0 1 1) and (2 0 0) atomic layers matches almost exactly. The twin-law above corresponds to a rotation of 60° around the *a*-axis (Fig. 1), and thus the twin has a pseudo-hexagonal symmetry. The twin results from a rotation of a grain by 60° around the [1 0 0] axis when the crystal is pulled on the Czochralski furnace, so that the growth direction originally parallel to the *c*-axis becomes parallel to [0 1 1]. We have found that the same twinning occurs in other $ThMn_{12}$ type compounds, namely $LuFe_4Al_8$ and $HoFe_4Al_8$ that we have recently examined with neutrons. The occurrence of such twinning was never described in the literature, to our knowledge, although the occurrence of hexagonal structures in close relation with $ThMn_{12}$ type of structure is well known [18,19] (e.g., UFe_6Ge_6 crystallises in one of these hexagonal structures [20]). We have successfully used the twin-law to refine the crystal structure from the neutron intensities, using the twinning refinement option of the least-squares program SHELXL93 [21]. The whole set of 2762 reflections was used in the refinement that includes as an additional parameter the fraction volume of the two grains A and B of the twin. For each reflection the contribution of the two grains is calculated and included in the least-squares matrix. The refinement converged within a few cycles to an *R*-factor of 8.7%, with the results shown in Table 3. The refined volume fraction of the grains is 82(1) : 18(1)% and the refined structural parameters are in good agreement with those derived from the X-ray data. In order to refine the site occupancies we have started from a 50% occupancy of Fe and

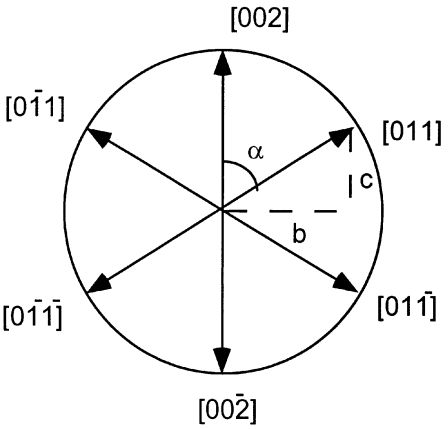

Fig. 1. The rotation of $\alpha = 60°$ around the *a*-axis (perpendicular to the plane of the drawing) that explains the twin-law observed in UFe_6Al_6. Such a rotation transforms [1 0 1] → [0 0 2] if $b(= a) \approx \sqrt{3}c$.

Table 3
Results of the structure refinement from the neutron data. Parameters defined as in Table 2

Atom	Position	*x*	*y*	*z*	OF	$U \times 10^2$ (Å^2)
U	2a	0	0	0	1(fixed)	0.84(3)
Fe	8f	1/4	1/4	1/4	1.02(2)	0.64(2)
Al	8f	1/4	1/4	1/4	0.00(2)	0.64(2)
Fe	8j	0.2750(2)	1/2	0	0.44(2)	1.51(5)
Al	8j	0.2750(2)	1/2	0	0.56(2)	1.51(5)
Fe	8i	0.3439(3)	0	0	0.00(2)	0.79(5)
Al	8i	0.3439(3)	0	0	1.00(2)	0.79(5)

Al on the 8i, 8j and 8f sites, deliberately far away from the X-ray values, in order to test the robustness of the least-squares procedure. A restraint on the least-squares refinement was imposed so that the sum of the occupancies of the Fe and Al atoms at each site is 100(2)% and that the total Fe and Al content correspond to the stoichiometry within 2%. We have tested that such restraints do not give a significantly different result from an unrestrained refinement, but just help the least-squares cycles to converge faster.

Two different samples were studied by ^{57}Fe Mössbauer spectroscopy: (i) a fragment of the $UFe_{5.8}Al_{6.2}$ polycrystalline material obtained by induction melting and (ii) a small piece of a grown single-crystal. Both materials were crushed and suitable amounts of the resulting powders were pressed together with lucite powder into perspex holders in order to obtain two homogeneous and isotropic Mössbauer absorbers containing $\approx 5\,mg\,cm^{-2}$ of natural iron. ^{57}Fe Mössbauer measurements were performed in transmission mode using a conventional constant acceleration spectrometer and a 25 mCi ^{57}Co source in Rh matrix. The velocity scale was calibrated using an α-Fe foil at room temperature. Spectra were collected between 321 and 5 K. Low temperature spectra were obtained using a liquid nitrogen/liquid helium flow cryostat (temperature stability ± 0.5 K). The spectra were fitted to Lorentzian peaks using a modified version of the non-linear least-squares computer method of Stone [22].

Magnetic measurements were performed on oriented single crystals with approximate dimensions $1.0 \times 0.7 \times 0.2\,mm^3$, using a SQUID magnetometer (Quantum Design, MPMS). The measurements were performed for magnetic fields in the range -5.5 to 5.5 T and for temperatures between 2 and 400 K.

3. Results and discussion

The single crystal X-ray diffraction data are in agreement with previous powder measurements [23], that indicate a $ThMn_{12}$-type structure for the $UFe_{5.8}Al_{6.2}$ polycrystalline sample ($a = 8.6744(3)$ Å, $c = 5.0142(3)$ Å). The present refinement clearly shows that the iron atoms occupy all the 8f and less than one half of the 8j crystallographic positions, converging to a $UFe_{5.6}Al_{6.4}$ composition. Average numbers of nearest neighbours and interatomic distances for the various positions obtained in the X-ray refinement are listed in Table 4. The X-ray powder results also confirm this type of structure in the pulled single crystals, with no signs of extra peaks.

Despite the twinning, the refined occupancies from the neutron-data are probably more accurate than those given by X-rays, due to the fact that Al and Fe scatter X-rays much less than uranium, which is not the case with neutrons. The higher R-value from the neutron refinement, that could partially be attributed to disorder at the

Table 4
$UFe_{5.8}Al_{6.2}$ interatomic distances (d) and nearest neighbours (NN) average numbers

	NN	Atoms	d (Å)		NN	Atoms	d (Å)
U(2a)	8	Fe(8f)	3.313	Fe(8f)	2	Fe(8f)	2.507
	8	(Fe,Al)(8j)	3.161		4	(Fe,Al)(8j)	2.516
	4	(Fe,Al)(8i)	2.990		4	(Fe,Al)(8i)	2.636
					2	U(2a)	3.313
(Fe,Al)(8j)	4	Fe(8f)	2.516	(Fe,Al)(8i)	4	Fe(8f)	2.636
	2	(Fe,Al)(8j)	2.723		2	(Fe,Al)(8j)	2.724
	2	(Fe,Al)(8i)	2.724		2	(Fe,Al)(8j)	2.762
	2	(Fe,Al)(8i)	2.762		1	(Fe,Al)(8i)	2.694
	2	U(2a)	3.161		4	(Fe,Al)(8i)	3.149
					1	U(2a)	2.990

grain boundaries, should not invalidate this statement.

Significant differences were found in the Mössbauer spectra of $UFe_{5.8}Al_{6.2}$ polycrystalline samples obtained by arc melting and of the grown single crystals. For the $UFe_{5.8}Al_{6.2}$ polycrystalline sample the Mössbauer spectra obtained between 321 and 310 K (Fig. 2) consist of a quadrupole doublet overlapping a broad absorption band. This absorption band may be fitted by a distribution of hyperfine fields, B_{hf}. This distribution was simulated by a sum of 10 magnetic splittings with the same isomer shift and quadrupole shift corresponding to a set of $10B_{hf}$ values; during refinement the difference between two consecutive B_{hf} values was 1 T and the width of all the Lorentzians in the B_{hf} distribution was kept equal. As the temperature decreases the relative area of the B_{hf} distribution increases at the expense of the quadrupole doublet (Table 5). At 296 K only a broad absorption band is observed. The spectrum obtained at 78 K was analysed considering two magnetic sextets with broad peaks corresponding to Fe atoms on two crystallographic sites 8f and 8j. The relative areas of peaks 1–6/2–5/3–4 of each sextet were constrained to be equal to 2.7/1.9/1.0 in order for the fitting process to converge. Furthermore, the half-widths of lines 1–6, 2–5 and 3–4 of each magnetic splitting were constrained to remain equal. Although the fit is poor (Fig. 2) the parameters estimated from this analysis (Table 5) are the same as those published by Recko et al. [10], within experimental error. Considering the estimated relative areas and the site occupation factors deduced from X-ray diffraction (Table 2), the assignment of these sextets to Fe on the 8f and 8j sites is also the same as in Ref. [10].

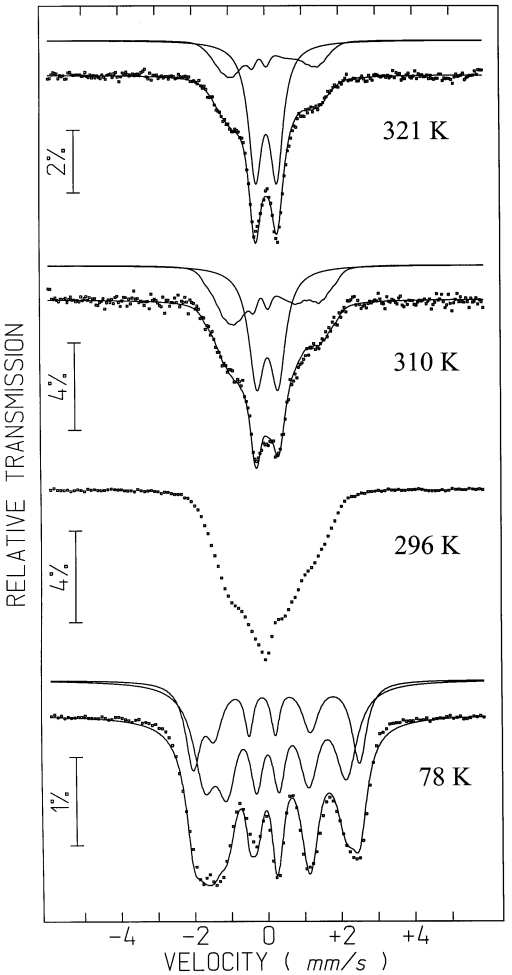

Fig. 2. Mössbauer spectra of the polycrystalline sample with nominal composition $UFe_{5.8}Al_{6.2}$ taken at different temperatures. The calculated function is represented on the experimental points. Slightly shifted the calculated subspectra are also shown.

In contrast to the results obtained with the polycrystalline material, the Mössbauer spectrum of the crushed single crystalline sample obtained at 296 K (Fig. 3) consists only of a slightly asymmetric doublet indicating that all the Fe in this material still shows paramagnetic behaviour. The results of the best fit obtained assuming two quadrupole splittings (corresponding to Fe atoms on the 8f and on the 8j sites) are summarised in Table 3. At 293 K the absorption peaks start to broaden (Fig. 3) which is consistent with the onset of magnetic ordering as indicated by magnetisation measurements discussed below. At 78 and 5 K similar spectra with six resolved peaks are observed (Fig. 3). These spectra may be fitted by two sextets in the same way as the 78 K spectrum of the polycrystalline material. The final fits obtained for the spectra of the single-crystalline material (Fig. 3) are better than that obtained in the previous case (Fig. 2).

The differences between the two types of samples suggest a higher degree of disorder of the polycrystalline material. On the other hand, it should be

Table 5
Estimated parameters from the Mössbauer spectra of the $UFe_{5.8}Al_{6.2}$ samples: (i) fragment of the polycrystalline material obtained by induction melting and (ii) small piece of a grown single-crystal. δ isomer shift relative to metallic α-Fe at 300 K; Δ quadrupole splitting measured in the paramagnetic rate; $\varepsilon = (e^2 V_{ZZ} Q/4)(3\cos^2\theta - 1)$ quadrupole shift calculated from $(\phi_1 + \phi_6 - \phi_2 - \phi_5)/2$ where ϕ_n is the shift of the nth line of the magnetic sextet due to quadrupole coupling. B_{hf} magnetic hyperfine field. I relative areas. Estimated errors are ± 0.3 T for B_{hf} and ± 0.02 mm/s for δ, Δ and ε

Sample	T (K)	site	δ (mm/s)	Δ (mm/s)	ε (mm/s)	B_{hf} (T)	I (%)
(i)	321	8f, 8j	0.08	0.59	–	–	66
			0.014	–	0.28	7.8[a]	34
	310	8f, 8j	0.09	0.59	–	–	52
			0.05	–	0.28	7.8[a]	48
	78	8f	0.21	–	0.21	12.0	68
		8j	0.13	–	0.41	14.1	32
(ii)	296	8f	0.05	0.63	–	–	68
		8j	0.18	0.57	–	–	32
	78	8f	0.20	–	0.27	13.1	68
		8j	0.27	–	0.29	10.1	32
	5	8f	0.21	–	0.28	13.7	70
		8j	0.28	–	0.27	10.7	30

[a]Average value of the B_{hf} estimated from a magnetic hyperfine field distribution.

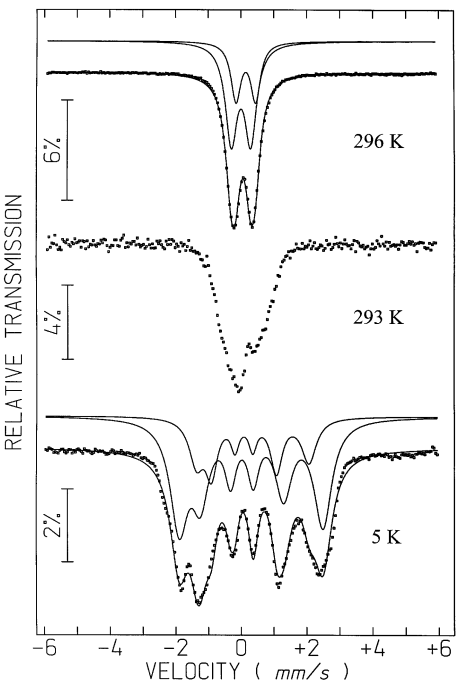

Fig. 3. Mössbauer spectra of the single-crystalline sample $UFe_{5.8}Al_{6.2}$ taken at 296 and 293 K emphasizing the magnetic ordering transition and at 5 K in the magnetic ordered state.

emphasised that the only way to fit the spectra of the single-crystalline material is to consider that the magnetic sextet with higher relative area has also the higher B_{hf} in contrast to what was observed for the polycrystalline samples. Comparing the relative areas of these magnetic sextets (Table 5(i)) with site occupation factors from neutron data, the Fe atoms on the 8f site should have a higher magnetic moment than those on the 8j sites as opposed to what has been generally admitted based on data from samples obtained by arc or induction melting. Large line-width values (decreasing from the external to the inner lines of each sextet $\Gamma_{1,6} > \Gamma_{2,5} > \Gamma_{3,4}$) are however still observed; they are due to the narrow distribution of B_{hf} at the Fe nuclei on each crystallographic site resulting from the random occupation of the 8j sites by both Al and Fe. This random occupation of the 8j sites by two different kinds of atoms implies several configurations of the Fe local environment, with different numbers of Al nearest neighbours. Since the hyperfine fields depend both on the crystallographic site and on the number of Al nearest neighbours, the B_{hf} distributions may therefore be explained by the atomic disorder in the local environment of the Fe atoms on each site.

The temperature dependence of the magnetisation under different magnetic fields both for zero field cooling (ZFC) and field cooling (FC) procedures is shown in Fig. 4. The $UFe_{5.8}Al_{6.2}$ presents a ferromagnetic behaviour below 300(1) K. This transition is confirmed by AC susceptibility measurements that show a peak at 295(2) K. For higher temperatures a Curie–Weiss law behaviour is followed, with $\theta = 304(2)$ K. This transition temperature is significantly lower than those previously reported for UFe_6Al_6 from powder magnetisation and Mössbauer measurements: 355 K [11], 334 K (Table 1 in Ref. [24]), 350 K [10]. These discrepancies only partially can be due to the slightly lower iron content of the single crystal and most certainly reflects the inhomogeneities of the polycrystalline samples. This is supported by the analysis of the Mössbauer spectra for the polycrystalline sample with $UFe_{5.8}Al_{6.2}$ nominal composition obtained in this work by induction melting (Table 5): at 321 K (the highest temperature measured) the spectrum indicates that either a significant amount of the material is already magnetically ordered or strong spin correlations which freeze the Fe magnetic moments in the Mössbauer time scale exist in the material. However, a paramagnetic doublet is also clearly observed down to 310 K. This paramagnetic doublet is similar to the one observed in the spectrum of the single-crystalline material above $T_C = 295$ K (Table 5). Thus, different magnetic ordering temperatures seem to be found for the polycrystalline sample and can be ascribed to a mixture of different compositions within this material. In this sense it is important to mention that the X-ray refinement of the small single-crystal extracted from the polycrystalline sample with $UFe_{5.8}Al_{6.2}$ nominal composition also indicates a lower Fe content ($UFe_{5.6}Al_{6.4}$, cf. Table 2), implying an inhomogeneous Fe distribution in this sample.

Single crystal magnetisation measurements along the different crystallographic axes revealed a basal type anisotropy, in agreement with the previous powder neutron diffraction results [10]. The *a* and *b* axes are the easy directions, the magnetisation curves with the field parallel to these axes presenting a typical ferromagnetic behaviour (Fig. 5). Along these directions, the saturation is reached for fields ~ 1.5 T, while the measurements performed with applied fields parallel to the *c* hard direction show a linear variation of the magnetisation with field, without saturation up to 5.5 T. The magnetic anisotropy of the compound is relatively high, with a predicted anisotropy field (given by the interception of the extrapolation of the hard direction magnetisation curve with the easy one) of ~ 27 at 5 K.

From the 5 K hysteresis curve for fields along the easy direction (*a*) a remanent magnetisation, $M_R = 6.5\ \mu_B$/f.u., and a coercive field, $H_c = 0.15$ T, are

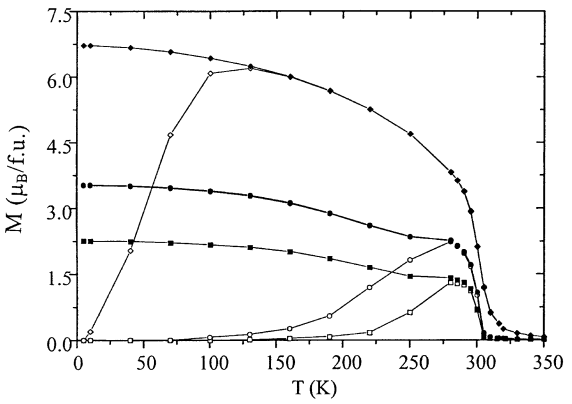

Fig. 4. Magnetization of $UFe_{5.8}Al_{6.2}$ single crystal along *a* (easy axis), as a function of temperature at fields (open symbols: zero field cooled mesurements; closed symbols: field cooled measurements; diamonds: 1000 Oe, circles: 100 Oe, squares: 50 Oe).

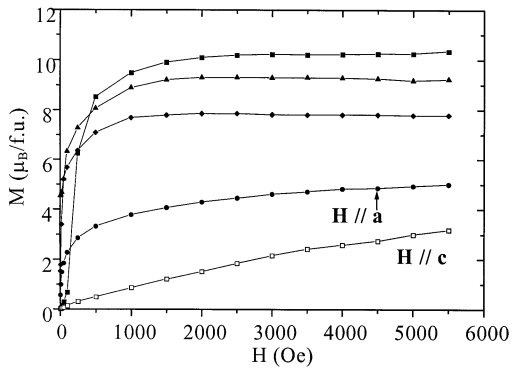

Fig. 5. Magnetization of $UFe_{5.8}Al_{6.2}$ single crystal as a function of the magnetic field along *a* (closed symbols) and *c* (open symbols) axes at different temperatures (squares: 5 K, triangles: 100 K, diamonds: 200 K, circles: 300 K).

deduced. The variation of the remanent magnetisation, M_R, and spontaneous magnetisation, M_S (obtained from the extrapolation of the easy direction magnetisation curve to $H = 0$) with temperature is presented in Fig. 6. These two quantities decrease with increasing temperature, the remanent magnetisation becoming negligible above 250 K and the spontaneous magnetisation decreasing from 10.4 μ_B/f.u. at 5 K to 6.5 μ_B/f.u. at 250 K. The coercive field also decreases with increasing temperature (Fig. 7) following an exponential decay as expected for a simple ferromagnet:

$$\ln(H_c) = aT + b$$

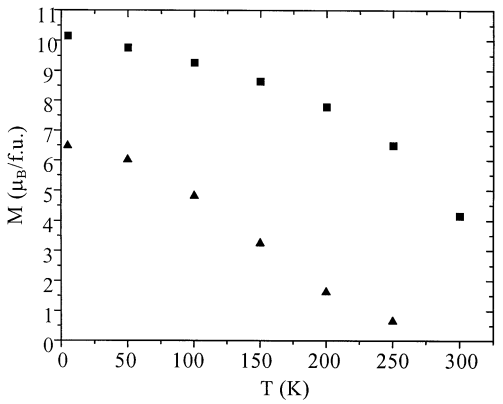

Fig. 6. Remanent and saturation magnetization of $UFe_{5.8}Al_{6.2}$ single crystal along the easy axis *a*, as a function of temperature.

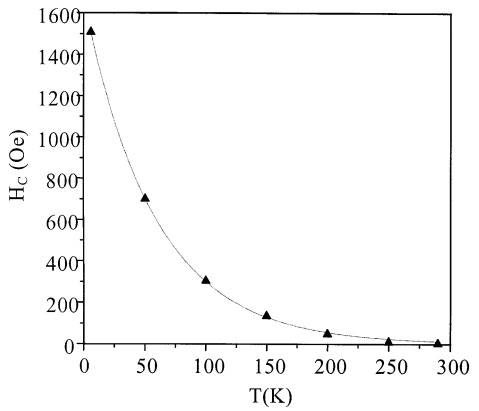

Fig. 7. Coercive field as a function of temperature, for $UFe_{5.8}Al_{6.2}$ single crystal with applied field along the easy axis *a*.

with $a = -0.0179$ and $b = 7.442$ and a 0.998 correlation coefficient.

At low fields and for measurements with $T < 100$ K, the easy direction $M(H)$ curves at lower temperatures show lower initial susceptibility values (see Fig. 5). A similar behaviour was previously observed in $UFe_{10}Mo_2$ single crystal magnetisation measurements [25]. This behaviour can be explained as a consequence of domain rotation in a basal plane anisotropy system. Considering that the *a* and *b* axes are the only easy magnetisation directions, at zero field there is an equal number of domains oriented along these two directions. At very low fields only the domains oriented parallel to the field contribute to the magnetisation; with the increase of the field, a critical value is reached for which the domains oriented perpendicular to the field will start to rotate towards the parallel configuration, contributing to the magnetisation. This effect becomes less pronounced at higher temperatures due to an easier domains rotation.

Pronounced differences between the temperature dependence of the zero field cooled and field cooled magnetisation curves are observed at low temperatures along the *a* easy axis, similarly to the case of UFe_4Al_8 crystals [26]. However, these differences are, in this case, one order of magnitude smaller. This is probably due to the lower magnetic anisotropy in the higher iron content compound (estimated anisotropy field of the order of 27 T at 5 K), when compared with the UFe_4Al_8, where the anisotropy field is predicted to be above 50 T.

4. Conclusions

In conclusion, these single crystal magnetisation measurements confirm $UFe_{5.8}Al_{6.2}$ as a ferromagnet with a basal plane type anisotropy, as previously suggested by powder neutron diffraction results. The large magnetic anisotropy suggests a significant contribution from the uranium atoms. However, this contribution cannot be clearly established without single crystal neutron diffraction experiments in untwinned samples. The comparison of the magnetic behaviour of this compound with the UFe_4Al_8 single crystal results allows to conclude that not only the Curie temperature is strongly

dependent on the iron content of the sample but also the partial substitution of the 8j site by iron dramatically changes the magnetic interactions between the iron atoms from antiferro to ferromagnetic.

Acknowledgements

This work was partially supported by NATO through Collaborative Research Grant No. 920996 and by JNICT (Portugal) under contract PRAXIS/3/3.1/FIS/29/94. J.A. Paixão is indebted to the European Commission for support for their experiments at Siloë and Risø on the framework of the Large Installation Programme. We thank Bente Lebech for giving us the opportunity to test the crystals at Risø and Manuela Silva for her help at Risø and on the X-ray powder diffractometry.

References

[1] H.S. Li, J.M.D. Coey, in: K.H.J. Buschow (Ed.), Handbook of Magnetic Materials, vol. 6, North-Holland, Amsterdam, 1991, p. 1.
[2] K.H.J. Buschow, in: G.J. Long, F. Grandjean (Eds.), Supermagnets, Hard Magnetic Materials, Kluwer, Dordrecht, 1991, p. 49.
[3] K.H.J. Buschow, A.M. van der Kraan, J. Phys. F 8 (1978) 921.
[4] I. Felner, I. Nowik, J. Phys. Chem. Solids 39 (1978) 951.
[5] A. Baran, W. Suski, T. Mydlarz, J. Less-Common Met. 96 (1984) 269.
[6] A. Baran, W. Suski, T. Mydlarz, Physica B 130 (1985) 219.
[7] J.A. Paixão, S. Langridge, S.Aa. Sørensen, B. Lebech, A.P. Gonçalves, G. Lander, P.J. Brown, P. Burlet, E. Talik, Physica B 234–236 (1997) 614.
[8] G. Bonfait, M. Godinho, P. Estrela, A.P. Gonçalves, M. Almeida, J.C. Spirlet, Phys. Rev. B 53 (1996) R480.
[9] J.A. Paixão, B. Lebech, A.P. Gonçalves, P.J. Brown, G.H. Lander, P. Burlet, A. Delapalme, J.C. Spirlet, Phys. Rev. B 55 (1997) 14370.
[10] K. Recko, M. Biernacka, L. Dobrzynski, K. Perzynska, D. Satula, K. Szymanski, J. Waliszewski, W. Suski, K. Wochowski, G. André, F. Bourée, J. Phys.: Condens. Matter 9 (1997) 9541.
[11] B. Ptasiewicz-Bak, A. Baran, W. Suski, J. Leciejewicz, J. Magn. Magn. Mater. 76&77 (1988) 439.
[12] A.P. Gonçalves, M. Almeida, C.T. Walker, J. Ray, J.C. Spirlet, Mater. Lett. 19 (1994) 13.
[13] A.C.T. North, D.C. Phillips, F.S. Mathews, Acta Crystallogr. A 24 (1968) 351.
[14] J.O. Lundgren, Crystallographic Computer Programs, Rep. UUIC-B13-04-05, Institute of Chemistry, University of Uppsala, 1982.
[15] J.A. Ibers, W.C. Hamilton (Eds.), International Tables for X-Ray Crystallography, vol. 4, Revised and Supplementary Tables, Kynoch, Birmingham, 1974.
[16] J.P. Becker, P. Coppens, Acta Crystallogr. A 30 (1974) 129.
[17] J.P. Becker, P. Coppens, Acta Crystallogr. A 31 (1975) 417.
[18] B. Chafik El Idrissi, G. Venturini, B. Malaman, Mater. Res. Bull. 26 (1991) 1331.
[19] B. Chabot, E. Parthé, J. Less-Common. Met. 93 (1983) L1.
[20] A.P. Gonçalves, J.C. Waerenborgh, G. Bonfait, A. Amaro, M.M. Godinho, M. Almeida, J.C. Spirlet, J. Alloys Compounds 204 (1994) 59.
[21] G.M. Sheldrick, SHELXL93. Program for Refinement of Crystal Structures, University of Göttingen, Germany, 1993.
[22] J.C. Waerenborgh, F. Teixeira de Queiroz, LNETI, ICEN, Research Rep., 1984.
[23] A. Baran, W. Suski, O.J. Zogal, T. Mydlarz, J. Less-Common Met. 121 (1986) 175.
[24] F.G. Vagisov, W. Suski, K. Wochonowski, H. Drulis, J. Alloys Compounds 219 (1995) 271.
[25] P. Estrela, M. Godinho, A.P. Gonçalves, M. Almeida, J.C. Spirlet, J. Magn. Magn. Mater. 167 (1997) L185.
[26] M. Godinho, G. Bonfait, A.P. Gonçalves, M. Almeida, J.C. Spirlet, J. Magn. Magn. Mater. 140–144 (1995) 1417.